Calculation of Activities of Ions in Molten Salts with Potential Application to the Pyroprocessing of Nuclear Waste

Mathieu Salanne, Christian Simon, and Pierre Turq

Université Pierre et Marie Curie-Paris6, CNRS, ESPCI, UMR 7612, Laboratoire LI2C, Case Courrier 51, 4 Place Jussieu, 75252 Paris Cedex 05, France

Paul A. Madden*

School of Chemistry, University of Edinburgh, Edinburgh EH9 3JJ, United Kingdom

Received: July 7, 2007; In Final Form: September 24, 2007

The ability to separate fission products by electrodeposition from molten salts depends, in part, on differences between the interactions of the different fission product cations with the ions present in the molten salt "solvent". These differences may be expressed as ratios of activity coefficients, which depend on the identity of the solvent and other factors. Here, we demonstrate the ability to calculate these activity coefficient ratios using molecular dynamics simulations with sufficient precision to guide the choice of suitable solvent systems in practical applications. We use polarizable ion interaction potentials which have previously been shown to give excellent agreement with structural, transport, and spectroscopic information of the molten salts, and the activity coefficients calculated in this work agree well with experimental data. The activity coefficients are shown to vary systematically with cation size for a set of trivalent cations.

I. Introduction

The Generation IV International Forum (GIF)[1] consists of a consortium of ten nations which is planning the nuclear reactors of tomorrow (2015−2030). Six reactor concepts have been chosen and research and development programmes have been initiated. The reprocessing of the nuclear waste to minimize environmental impact, radiotoxicity, and proliferation risk is an integral part of each reactor project.[2] Several nations in Europe, Asia, and the U.S.A. are investigating "pyroprocessing" as the preferred means of dealing with this waste. As schematically illustrated in Figure 1, pyroprocessing involves the electrochemical reduction of the spent fuel rods in a molten salt electrolyte to selectively deposit the radioactive waste elements as metals or alloys at appropriately chosen cathodes. The potential advantages of this technology over current solvent−solvent extraction processes[3] are that they may be used on radioactively "hot" fuels, which degrade the organic solvents and chelating agents used in solvent extraction, thereby allowing reprocessing on a short time scale after emergence from the reactor. Also, they involve smaller volumes of solvent, reducing environmental risks, and they may be tailored to extract quantitatively all the radioactive fission products, for recycling, disposal, or transmutation as appropriate. These characteristics mean that reprocessing can be made an integral element of reactor operation, reducing proliferation risks. A closed cycle for the consumption of all fissionable material is a feature of the proposed molten salt reactor, for example.[4]

In this article, we report the development of theoretical methods which predict the effect of the choice of electrolyte on the separability of different metal ions by pyroprocessing. We demonstrate the capability in calculations on a series of trivalent metal ions in a molten salt "solvent", the much used LiCl/KCl mixture at the eutectic composition. The selected ions span a range of cation ionic radii which would contain the (trivalent) fission products of practical interest. We will show that the separability may be related to ratios of activity coefficients for different cations. These activity coefficients reflect the interactions between the cations and the other ions present in the electrolyte; in the case we will consider these will be dominated by the interactions with the first coordination shell of Cl^- ions. The central issue then becomes one of predicting differences between free energies of solvation of

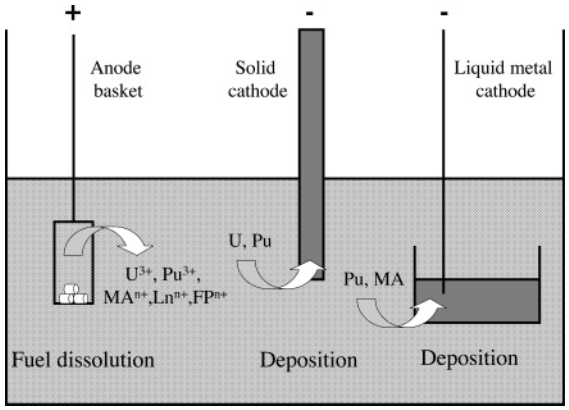

Figure 1. Schematic view of pyroprocessing of nuclear fuel waste. The spent fuel rods are placed in an anode basket, and the fuel elements, U and Pu, together with "minor actinide" (MA) and other lanthanides (Ln) and "fission products" (FP) are dissolved in the melt. In the cell illustrated, there are two cathodes to indicate that different cathode materials may be used to increase the selectivity of the electrodeposition process. In a first step, U and Pu can be deposited on a solid metal electrode, and in a second step, the remaining Pu is extracted with the minor actinides (MA) in a liquid metal phase. Lanthanides and fission products remain in the molten salt during this process.

* Corresponding author.

10.1021/jp075299n CCC: $40.75
Published on Web 01/05/2008

different cations, a problem which has been examined by simulation in aqueous systems, especially in the biochemical context[5] but which has not been considered in the more strongly interacting ionic fluids of interest here. The development of predictive theoretical methods will minimize the experimental effort required to optimize the electrolyte in developing the reprocessing technology. This is an important consideration because there are severe practical constraints on the ability to perform a broad range of experiments to fully characterize the physicochemical properties of these systems as the range of possible solvents is spanned. The melts themselves are at high temperatures and are highly corrosive, but more significantly, they contain radioactive elements so the experiments must be carried out under conditions of security which very much limits the number of laboratories where the experiments may be performed. It will be useful to establish some basic principles through the simulations to guide the choice of most appropriate coordinating anions and to correlate the results of the limited set of experiments which may be performed.

The theoretical development has involved the refinement of interaction potentials which allow a realistic description of the materials of interest and which have previously been shown to give excellent reproduction of structural, spectroscopic, and transport properties of these melts.[6−8] These potentials are polarizable, and parameters which control the short-range repulsion as well as the polarization effects have been shown to depend systematically on the radius of the cation. Here, we show how these potentials may be used in thermodynamic integration schemes with sufficient statistical precision to reproduce the differences between the activity coefficients which control the separability of different elements using the pyroprocessing methods.

We begin by illustrating how the separability may be related to thermodynamic properties of the ions involved and then how these properties may be calculated from a computer simulation. We emphasize the need for a practical scheme which allows the statistical precision necessary to obtain the ratios of activity coefficients accurately, as this involves calculating the difference between similar quantities. In the final section, we compare results with measurements which have been made for the selected ions in the LiCl/KCl eutectic mixture and discuss the prospects for rendering such calculations on other materials and in different solvents on a completely predictive, first-principles basis.

II. Principles of Separation by Electrodeposition

The electrochemical reaction involved in the deposition of some metal (M) is

$$M^{n+}(\text{solvent}) + ne^- \rightarrow M(\text{cathode}) \tag{1}$$

where M^{n+}(solvent) is the dissolved metal in the ionic liquid solvent and M(cathode) is the metal as deposited on the cathode surface: many of the waste products of interest (including lanthanides and most actinides) adopt an oxidation state of $n = 3$ in a chloride melt such as the eutectic mixture of LiCl and KCl. Li/KCl is a typical solvent system for electrodeposition studies, and it is the system we will use in the calculations described below. According to Nernst's Law, the concentration of the metal ions present at equilibrium, when an electrical potential E is applied to the cell, is determined by

$$E = E^0_{M^{3+}/M} + \frac{RT}{3F}\ln[a_{M^{3+}}] \tag{2}$$

where $E^0_{M^{3+}/M}$ is a standard electrode potential, and may be regarded as the potential at which the cell would be at equilibrium if it contained pure molten MCl_3, rather than a solution of MCl_3 in Li/KCl. The second factor accounts for the change in the free energy of the M^{3+} ions by virtue of their dissolution in Li/KCl with their activity $a_{M^{3+}}$ expressed in terms of the mole fraction $x_{M^{3+}}$ by

$$a_{M^{3+}} = \gamma_{M^{3+}} x_{M^{3+}} \tag{3}$$

Here $\gamma_{M^{3+}}$ is an activity coefficient which reflects the interactions of M^{3+} ions with the Li/KCl solvent. Equation 2 also contains the gas and Faraday constants R and F and the absolute temperature T. It is then useful to introduce an apparent standard potential, which is now solvent dependent,

$$E'^0_{M^{3+}/M} = E^0_{M^{3+}/M} + \frac{RT}{3F}\ln[\gamma_{M^{3+}}] \tag{4}$$

This is the quantity measured experimentally, and it enables us to compare electrode potentials for different metals at the same concentration in the solution conditions. Equations 2 and 4 show that if the potential applied to a cell initially containing a concentration $x^{\text{initial}}_{M^{3+}}$ metal ions is slowly increased to a value somewhat larger than E'^0 effectively all of the metal ions will be removed from the solvent and deposited on the cathode.

The key factor to be assessed is the ability to separately deposit different metallic species. Suppose the solvent contains two trivalent metals M and N with the latter having the larger value for E^0, and for simplicity, suppose that they have the same initial concentrations $x^{\text{initial}}_{M^{3+}} = x^{\text{initial}}_{N^{3+}}$; then, to be able to separate M from N, we require that the potential on the cell may be increased to a value by which effectively all of the M^{3+} ions have been removed, reaching the very low concentration $x^{\text{final}}_{M^{3+}}$, before the electrodeposition of N begins. The separability may be expressed in the ratio

$$\eta = 1 - \frac{x^{\text{final}}_{M^{3+}}}{x^{\text{initial}}_{M^{3+}}} \tag{5}$$

By applying the Nernst equation to both M and N when a given potential E is applied to the cell, we can see that

$$\frac{x_{M^{3+}}}{x_{N^{3+}}} = \frac{\gamma_{N^{3+}}}{\gamma_{M^{3+}}}\exp\left[-\frac{3F(E^0_{M^{3+}/M} - E^0_{N^{3+}/N})}{RT}\right] \tag{6}$$

Hence, by setting $x_{M^{3+}} = x^{\text{final}}_{M^{3+}}$ and $x_{N^{3+}} = x^{\text{initial}}_{N^{3+}} = x^{\text{initial}}_{M^{3+}}$, we can relate the separability η when there are two metals present to the material properties

$$\eta = 1 - \frac{\gamma_{N^{3+}}}{\gamma_{M^{3+}}}\exp\left[-\frac{3F(E^0_{M^{3+}/M} - E^0_{N^{3+}/N})}{RT}\right] \tag{7}$$

If, to illustrate this relationship, we assume for the moment that the activity coefficients cancel and we require that M is 99.9% extractable (i.e. $\eta > 0.999$), this equation shows that the standard potentials of M and N must differ by more than 0.149 V at a temperature of 750 K.

More generally, eq 7 shows that there are two strategies which might be adopted to control the separability. The first is to change the cathode material, which may influence the difference between the standard potentials ($E^0_{M^{3+}/M} - E^0_{N^{3+}/N}$) since the metal when deposited may alloy with the cathode material which may shift the relative free energies of the deposited metal and

hence influence the electrode potentials.[9] Several cathode materials, including liquid as well as solid metals, as illustrated in Figure 1, have been examined. Currently, a cathode consisting of aluminum metal shows much promise.[10]

The second strategy is to change the electrolyte, which will affect the activity coefficients of different ions to different degrees. Simply changing the identity of the alkali ions is sufficient to have a substantial effect on the thermodynamic properties[11] of lanthanide cations, but more dramatic shifts could be induced by introducing polyvalent cations or introducing other anions, especially F^-. The importance of the solvent effect has been emphasized by recent experiments using a LiF/AlF_3 mixture as electrolyte.[12] By varying the composition of mixture, substantial shifts in the potentials at which different metals are deposited were detected.

A systematic way of predicting these solvent effects would be very valuable. Not only are there many solvent systems to be examined, but also the melts produced by dissolving spent fuel will contain many components, and their mutual separability must be considered. To sweep this parameter, space in laboratory experiments is unmanageable, especially when many of the elements of interest are hazardous radionucleides. Furthermore, there are other considerations which affect the solvent choice, such as operating temperature and corrosivity. Such constraints are particularly severe for the integrated reprocessing step in the molten salt reactor. Here, the molten salt is also the reactor fuel and must satisfy certain neutronic requirements too. A way of predicting the solvent performance from fundamental considerations becomes important to test whether separability of the key elements is even viable in the presence of these constraints. The other factor to be assessed, the difference of the standard potentials between different elements, is relatively easily obtained from experiment as it requires only one measurement on the pure melt of each metal.

Given an accurate description of the interactions between the ions, the activity coefficents could be obtained from computer simulation studies using thermodynamic integration methods to calculate appropriate free energies. For this to be successful, the model of the interactions between the constituent ions of the melts must be quantitatively accurate and must be obtainable from fundamental principles which allow a model to be generated for arbitrary multicomponent mixtures including ions for which very little experimental information is available, such as highly active radionucleides. Furthermore, for such interaction models, it must be possible to perform the thermodynamic integration with high statistical precision, in order that relatively small free energy differences between different species are correctly characterized: this implies relatively long thermodynamic integrations, requiring simulation runs which are beyond the scope of direct ab initio simulations.[13,14] We begin by describing the outcome of such calculations using suitably chosen interaction potentials and will return to the origin of the interaction model and its predictive capability at the end of the article.

III. Thermodynamic Integration

The activity could be obtained by performing a particle insertion,[15] using the so-called Kirkwood integration method. This has been successfully applied to calculate the solubility of KF and NaCl in water.[16,17] In this method, two or more particle insertions have to be performed: one in the system of interest and a second in a reference system (corresponding to a chemical potential of 0 for the species of interest). The chemical potential is obtained by subtracting the values of the work done in the insertion step. In our case, four particles would have to be inserted simultaneously (one M^{3+} or N^{3+} and three Cl^- ions) which is technically difficult because of the high densities of the melts involved and the strength of the interionic interactions. Alternatively, separate insertions of M^{3+} (or N^{3+}) and Cl^- ions could be attempted to obtain single ion activities. In this case, the simulation cell loses its neutrality and a system size-dependent correction term has to be added. As the inserted cation is trivalent, this term will be important and of the same order as the other contributions. Overall, the particle insertion method was not found to be a viable way of obtaining the requisite precision as it involves calculating the averages of several terms which are large because of the strength of the interactions in molten salts with the relatively small difference between them being the actual object of interest.

We chose to calculate the work required to transmute M^{3+} into N^{3+} instead. As in the insertion case, this procedure has to be applied in the system of interest, that is, a dilute solution of MCl_3 in the Li/KCl eutectic mixture, as well as in a reference system, for which we chose pure MCl_3 (NCl_3) liquid. Thus, the total thermodynamic transformation is:

$$MCl_{3,Li/KCl} + NCl_{3,pure} \rightarrow NCl_{3,Li/KCl} + MCl_{3,pure} \quad (8)$$

The total Gibbs' free energy (or reversible work) per cation associated with this transformation is related to the difference of activity coefficients between M^{3+} and N^{3+}:

$$\Delta G_{tot} = -RT \ln\left(\frac{\gamma_{MCl_3}}{\gamma_{NCl_3}}\right) \quad (9)$$

In our MD simulations, the two transformations to be performed are

$$MCl_{3,Li/KCl} \rightarrow NCl_{3,Li/KCl} \quad (10)$$

and

$$MCl_{3,pure} \rightarrow NCl_{3,pure} \quad (11)$$

The associated Gibbs' free energies are denoted ΔG_1 and ΔG_2. ΔG_{tot} is the difference between them ($\Delta G_{tot} = \Delta G_1 - \Delta G_2$), which means that we can access the difference of chemical potentials of MCl_3 and NCl_3 in Li/KCl by transformations between two similar systems and avoid the calculation of large free energy differences.

To calculate ΔG_i ($i = 1$ or 2), we performed molecular dynamics simulation in the NPT ensemble. We used the Kirkwood integration method in which a parameter (λ), which scales the interaction potential parameters, is introduced to define the progressive sliding from one thermodynamic state to another. For example, in the case of the transformation defined by eq 10, the starting state corresponds to a MCl_3 unit solvated in Li/KCl, for which $\lambda = 0$, and the final state corresponds to the same system in which the M^{3+} cation is replaced by a N^{3+}, and now $\lambda = 1$. For each value of λ, the interaction potential takes the form

$$U(\lambda) = (1 - \lambda)U_{MCl_3/LiKCl} + \lambda U_{NCl_3/LiKCl} \quad (12)$$

where $U_{MCl_3/LiKCl}$ is the set of interaction potentials describing all interactions between the M^{3+} ion and the other ions present in a mixture of MCl_3 and the LiCl/KCl solvent. The idea is illustrated in Figure 2 for a U^{3+} to Sc^{3+} transmutation. ΔG_1 is the sum of two terms, an ideal one that can be calculated

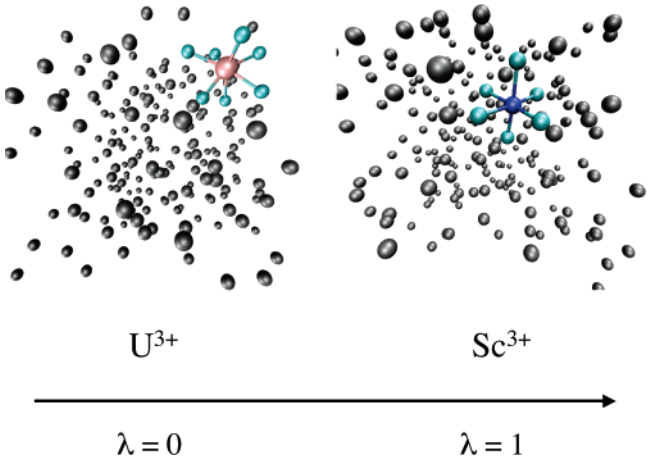

Figure 2. Schematic representation of the thermodynamic integration method. The two snapshots are taken from simulations of the initial ($\lambda = 0$ − U^{3+} in Li/KCl) and final ($\lambda = 1$ Sc^{3+} in Li/KCl) stages. The Cl^- ions which form the first coordination shells of the trivalent cations are connected to them with bonds, and the remaining ions illustrated are the Li^+, K^+, and Cl^- ions which make up the solvent. For intermediate values of λ, the trivalent metal ion corresponds to one intermediate between U^{3+} and Sc^{3+}. Note that the typical number of Cl^- ions coordinated to the trivalent species is larger for U^{3+} than for Sc^{3+}.

analytically:

$$\Delta G_1^{\mathrm{id}} = RT\left(\ln\left(\frac{N_N\Lambda_N{}^3}{\langle V(\lambda=1)\rangle}\right) - \ln\left(\frac{N_M\Lambda_M{}^3}{\langle V(\lambda=0)\rangle}\right)\right) \quad (13)$$

where Λ_M is the de Broglie thermal wavelength of element M, N_M is the number of ions transmuted, and V is the volume of the simulation cell, and a second term computed from

$$\Delta G_1^{\mathrm{res}} = \int_0^1 \left\langle \frac{\partial U(\lambda)}{\partial \lambda}\right\rangle_\lambda \mathrm{d}\lambda \quad (14)$$

Here, $\langle\cdots\rangle_\lambda$ means the average value of the quantity indicated in a simulation run in which the interaction potentials take on the intermediate value $U(\lambda)$, between the pure M and the pure N limits.

This kind of calculation is now routinely used in biochemical simulation[5] where, for example, the ion selectivity in potassium channels has been characterized in terms of free energy differences of the ions in the pore and in the bulk. In our case, the interaction potentials are polarizable and our description of the instantaneous state of the systems contains values for the instantaneous dipoles (μ) on each ion. In this case, the derivative of U with respect to λ is given by

$$\left\langle \frac{\partial U(\{\mu(\lambda)\};\lambda)}{\partial \lambda}\right\rangle_\lambda = \left\langle \sum_i \frac{\partial U(\{\mu(\lambda)\};\lambda)}{\partial \mu^i}\cdot\frac{\mathrm{d}\mu^i}{\mathrm{d}\lambda}\right\rangle_\lambda + \left\langle \frac{\mathrm{d}U(\{\mu(\lambda)\};\lambda)}{\mathrm{d}\lambda}\right\rangle_\lambda \quad (15)$$

However, because we obtain the instantaneous dipoles by a variational procedure, the derivative of the dipoles with respect to λ in the first term on the right-hand side may be ignored by virtue of the Hellmann−Feynman theorem and the remaining term is simply given by the difference between the analytic expressions for the interaction potentials with the dipoles taking their variationally optimized values. The integral is calculated by running simulations at several values of λ between zero and one and obtaining the integral numerically; this process is illustrated in Figure 3. In the transformation defined by eq 11 for the pure melts, all M^{3+} ions are transformed into N^{3+} ions, but the method used to compute ΔG_2 is the same as that described for ΔG_1; the only difference being that the calculated quantity must be divided by the number of MCl_3 units involved (N_M).

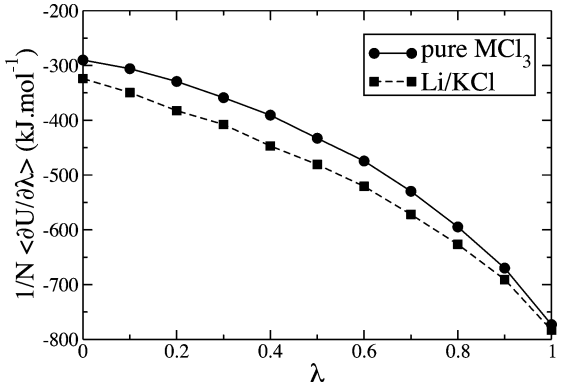

Figure 3. Values of $(1/N)\langle(\partial U/\partial\lambda)\rangle$ along the paths for transmutation of U^{3+} into Sc^{3+} in the pure liquid and in the solution are compared; see eq 14. Each point correspond to a 100 ps simulation, estimates of the statistical precision of the individual calculations gives error bars with widths equal to the size of the symbols used. Note that the integrals of the these two curves, which determine the free energies ΔG_1 and ΔG_2, will have similar values and that it is the difference between them which is of interest.

IV. Calculations and Comparison with Experiment

We have performed transformations involving five different trivalent cations: U^{3+}, La^{3+}, Y^{3+}, Tb^{3+}, and Sc^{3+}: as we shall discuss further below, this set spans a wide range of cation sizes, and the experiments to determine the electrodeposition potentials from pure melts and an LiCl/KCl eutectic mixture, which we require to check the method, have been performed on them. All of the simulations were performed in the NPT ensemble, where temperature and pressure were 750 K and 3×10^5 Pa, with the method described by Martyna et al.[18] For each system and each value of λ (taken from 0.0 to 1.0 by 0.1 steps, which corresponds to 11 simulations), 100 ps of dynamics were collected. The extracted values for $(1/N_{M,N})\langle(\partial U/\partial\lambda)\rangle$, corresponding to the transmutation of U^{3+} into Sc^{3+} in both Li/KCl and pure MCl_3 liquids, are represented versus λ on Figure 3. Runs of 100 ps were necessary to reduce the errors bars on the values appearing in the figure to the size of the symbols used to represent them. The integration of these curves then gives us the values of $\Delta G_1^{\mathrm{res}}$ and $\Delta G_2^{\mathrm{res}}$ for this transformation.

In this work, the variation of volume during the transformations was small because of the similarity of the systems involved, and the ideal term was then negligible compared with the second term, $\Delta G_i^{\mathrm{res}}$. A point of detail about the method proposed is that the use of a eutectic mixture for the electrolyte brings the operating temperature of a practical pyroprocessing system below the melting temperatures of the pure melts which are used as reference systems, so that these melts are in fact metastable with respect to crystallization at the temperature at which the thermodynamic integrations are performed. We therefore performed separate calculations on the reliability of the $\Delta G_2^{\mathrm{res}}$ values in which the transformation was performed well above the melting temperatures of both melts and the results for the free energy differences extrapolated to the temperature of interest by use of the Gibbs−Helmhotz equation of classical

TABLE 1: Calculated Gibbs' Free Energies[a]

M, N	ΔG_1	$-\Delta G_2$	ΔG_{tot} (sim)
La, Y	-282.3 ± 5.6	254.9 ± 5.1	-27.4 ± 10.7
La, Tb	-252.6 ± 5.0	228.5 ± 4.6	-24.1 ± 9.6
U, Y	-231.1 ± 4.6	204.2 ± 4.1	-26.9 ± 8.7
U, Sc	-503.0 ± 10.0	461.7 ± 9.2	-41.3 ± 19.2

[a] All the values are given in kilojoules per mole. Errors have been estimated by block averaging.

TABLE 2: Apparent Standard Potentials of the Various Redox Couples[a]

redox couple	E^0	$(RT/3F)\cdot \ln((\gamma_{M^{3+}}/\gamma_{La^{3+}}))$	E'^0_{calc}	E'^0_{exp}
M(III)/M(0)	(V)	(V)	(V)	(V)
U	0.65	0.00 ± 0.03	0.65 ± 0.03	0.63[b], 0.60[d], 0.65[e,f]
Sc	0.51	-0.14 ± 0.06	0.37 ± 0.06	0.30[b]
Tb	0.23	-0.08 ± 0.03	0.15 ± 0.03	0.14[c]
Y	0.20	-0.10 ± 0.03	0.10 ± 0.03	0.02[b], 0.02[e]
La	0.00	0.00	0.00	0.00

[a] La(III)/La(0) couple is taken as the reference. [b] Reference 20, $T = 723$ K. [c] Reference 21, $T = 873$ K. [d] Reference 22, $T = 733$ K. [e] Reference 23, $T = 723$ K. [f] Reference 24, $T = 723$ K.

thermodynamics. The results obtained showed a very small temperature dependence of ΔG_2^{res}, in perfect agreement with experimental findings.[19]

The values obtained for ΔG_1 and $-\Delta G_2$ for each transformation are given in Table 1. For all Gibbs' free energies calculated, we estimated relative errors of $\pm 2\%$ by block-averaging the statistical fluctuations in $\langle \partial U/\partial \lambda \rangle$. This leads to quite substantial error estimates for ΔG_{tot} because of the cancelation between ΔG_1 and ΔG_2. These numbers are likely to be an upper limit of the errors. They could be improved by longer thermodynamic integration runs and by avoiding the thermodynamic integration in the pure liquids at low temperatures where the structural relaxation times are long, perhaps by developing the Gibbs–Helmholtz idea. As we will see, the precision of the calculated apparent standard potentials is sufficient for the present purpose.

In order to compare our results to experimental ones, we computed the corresponding values of E'^0 with eq 4. The results are given in Table 2, in which the couple La(III)/La(0) was taken as a reference. Experimental points were determined by various electrochemical techniques such as cyclic voltammetry, chronopotentiometry, or electromotive force measurement; the references are given in the table caption.

We can see that the results are in good agreement with the experimental ones, despite a small overestimation of the apparent standard potentials of Y(III)/Y(0) and Sc(III)/Sc(0). We can observe a tendency for Sc, Tb, and Y to get smaller apparent standard potential differences with La upon solvation in Li/KCl eutectic relative to the corresponding standard potentials. U keeps a significant standard potential difference with respect to La, which is consistent with experimental observation. Thus, the results are excellent from a qualitative point of view, and they point out the fact that the solvation effects in Li/KCl tend to increase the separability of U(III) from lanthanides and other trivalent cations like Y^{3+} and Sc^{3+}, with the effect becoming more pronounced for smaller cations. From a quantitative point of view, the size of the calculated error does not allow us to consider our apparent standard values to be precise, but one should note that for most systems the estimated error (0.03 V) is considerably smaller than the critical value (0.149 V) required to get an efficiency of 99.9% for separating two elements. Moreover, the important case of the U(III)/U(0) couple shows that there is a significant discrepancy between various experimental studies used to obtain apparent standard potentials.

TABLE 3: Interaction Potential Parameters[a]

ion pair	B_{ij}	α_{ij}	C_{ij}^6	C_{ij}^8	b_{ij}^6	b_{ij}^8	b_{ij}^D	c_{ij}^D
$Cl^- - Cl^-$	100.0	1.53	222.26	7455.5	1.70	1.70		
$Cl^- - Li^+$	12.4	1.56	2.09	9.0	1.50	1.00	1.720	2.0
$Cl^- - K^+$	57.7	1.55	50.14	272.3	1.50	1.00	1.460	2.8
$Cl^- - Sc^{3+}$	175.0	1.80	30.03	300.0	1.56	1.05	1.390	1.0
$Cl^- - Y^{3+}$	273.0	1.80	41.51	450.0	1.50	1.00	1.336	1.0
$Cl^- - La^{3+}$	450.0	1.80	97.22	600.0	1.50	1.00	1.258	1.0
$Cl^- - Tb^{3+}$	283.8	1.80	53.90	800.0	1.50	1.00	1.317	1.0
$Cl^- - U^{3+}$	400.0	1.80	97.22	600.0	1.50	1.00	1.258	1.0
$Li^+ - Li^+$	2.0	1.57	0.08	0.1	1.5	1.0		
$Li^+ - K^+$	10.5	1.57	1.39	3.2	1.5	1.0		
$Li^+ - Sc^{3+}$	10.0	3.0	0.66	1.3	1.5	1.0		
$Li^+ - Y^{3+}$	10.0	3.0	0.90	2.1	1.5	1.0		
$Li^+ - La^{3+}$	10.0	3.0	1.91	3.3	1.5	1.0		
$Li^+ - Tb^{3+}$	10.0	3.0	1.13	2.4	1.5	1.0		
$Li^+ - U^{3+}$	10.0	3.0	1.91	3.3	1.5	1.0		
$K^+ - K^+$	54.5	1.56	25.38	89.5	1.5	1.0		
$K^+ - Sc^{3+}$	10.0	3.0	12.09	36.6	1.5	1.0		
$K^+ - Y^{3+}$	10.0	3.0	16.35	59.8	1.5	1.0		
$K^+ - La^{3+}$	10.0	3.0	34.80	94.6	1.5	1.0		
$K^+ - Tb^{3+}$	10.0	3.0	20.69	66.9	1.5	1.0		
$K^+ - U^{3+}$	10.0	3.0	34.80	94.6	1.5	1.0		
$Sc^{3+} - Sc^{3+}$	15.0	3.0	5.76	15.0	1.64	1.09		
$Y^{3+} - Y^{3+}$	15.0	3.0	10.53	40.0	1.5	1.0		
$La^{3+} - La^{3+}$	15.0	3.0	47.70	100.0	1.5	1.0		
$Tb^{3+} - Tb^{3+}$	15.0	3.0	16.87	50.0	1.5	1.0		
$U^{3+} - U^{3+}$	15.0	3.0	47.70	100.0	1.5	1.0		

[a] All values are given in atomic units. The Cl^- polarizability was set to 20 au.

V. Interaction Potentials

As the discussion of results in section IV makes clear, the system sizes and simulation run lengths necessary to obtain the necessary statistical precision makes the calculations well beyond what can be contemplated with ab initio molecular dynamics methods. Potentials must be introduced which are capable of reproducing the interactions sufficiently well that the thermodynamic properties of these materials are accurately reproduced. The interaction potentials used in this work are examples of "polarizable ion model" potentials.[6] Their form was suggested by ab initio electronic structure calculations on the interactions between the ions in a condensed-phase coordination environment, and some of the parameters, such as the ionic polarizabilities and those describing the dispersion interactions, were also obtained directly from first principles. The most significant interaction parameters, which govern the range of the repulsive interactions between the ions and the short-range contributions to the dipole induction, were refined so that the structures of the simulated pure MCl_3 liquids agreed with those seen in neutron and X-ray diffraction experiments.[6] It was found that a satisfactory generic interaction potential for a large set of such MCl_3 liquids could be found, where the differences between the parameter sets used for different materials could all be related to the crystallographic radius of the cation, this includes the short-range contributions to polarization as well as interionic repulsion. The transport and Raman spectroscopic properties of the simulated liquids were subsequently shown to be in excellent agreement with experiment.[7] When the potentials were applied to solutions of the MCl_3 liquids in Li/KCl mixtures, again, excellent results for the mixture densities, and X-ray absorption fine structure, transport, and spectroscopic properties were obtained.[8] They were thereby shown to be transferable, applicable to both the pure liquids and the solutions. The potentials used in the present work are detailed in Appendix.

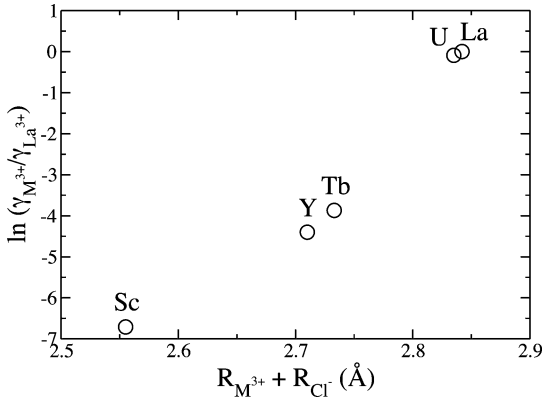

Figure 4. Correlation between the cation crystallographic radius ($R_{M^{3+}}$) and the calculated activity coefficient. The log of the activity is plotted versus the sum of the radii of the cation and a Cl^- ion. Values for radii from web elements.

The very good agreement that we have demonstrated between the calculated and measured activity coefficient ratios confirms that this potential is recapturing the essential features of the interactions of the trivalent metal ions with the electrolyte. Since the differences between interaction potentials for different systems are expressed solely through the cation size,[6] this suggests that the activity coefficients vary systematically with cation size, and this is confirmed in Figure 4, where we plot the logarithm of the activity coefficient versus the sum of the crystal radii of chloride with the cations. It will be a target of future work to obtain such relationships for different solvent systems, from simulation, and thus provide the information on which the technological process optimization can be based. The set of ions included in our selected set spans a very wide range of cation radii, within which almost all the trivalent lanthanide and actinide ions are found. This observation is not trivial since two of the members of the set (U^{3+} and Tb^{3+}) have partially filled f-electron subshells. It suggests that the effect of these unpaired electrons on the interactions between the cation and the electrolyte is adequately expressed with the same interaction model as used for the closed shell ions.

As we remarked in the Introduction, a full modeling capability would be predictive and not rely on the use of experimental information to parametrize the potentials. This becomes particularly important when the methods we have discussed are applied to the fluoride melts which are under active investigation for pyroprocessing in several countries.[25] Because of the difficulties of performing diffraction experiments on the highly corrosive fluoride melts, the type of structural information used to parametrize the chloride potentials used in the present work has not been obtained. However, we have recently developed a fully first-principles approach to the parametrization of interaction potentials of the type used in this work,[26,27] and the application of these methods to fluoride melts has been highly successful.[28,29] It should be a straightforward exercise to apply these methods to generate suitable potentials to fully explore the activities of polyvalent cations in such melts.

Acknowledgment. The authors would like to acknowledge the support of the European Commission's Research infrastructures activity of the Structuring the European Research Area program, Contract No. RII3-CT-2003−506079 (HPC-Europa). Financial support of PCR-RSF (program concerté de recherches - Réacteur à sels fondus) and GDR PARIS are gratefully acknowledged. We thank B. Rotenberg for helpful discussions.

Appendix: Computational Details

We carried out molecular dynamics simulations in the NPT ensemble[18] with a pressure of zero; the liquid densities which result with the chosen interaction potentials have previously been shown to agree well with experimental data. We fixed a time step of 0.5 fs to integrate the equations of motion, while the thermostat and barostat relaxation time were of 10 ps. In the case of pure MCl_3 liquids, the simulation cell contained 150 Cl^- and 50 M^{3+} ions, and in the case of the Li/KCl solutions, it contained 100 Cl^-, 56 Li^+, 41 K^+, and 1 M^{3+} ions. The form of the interaction potential, which includes polarization effect on the anion, is given in refs 6 and 27. Values for the induced dipoles at each step are obtained by minimizing the total interaction energy with respect to the dipole values using a conjugate gradient algorithm. The interaction potential consists of a pair potential of Born−Mayer form together with an account of interionic polarization. The pair potential is written

$$V(r_{ij}) = B_{ij}\, e^{-\alpha_{ij} r_{ij}} - f_{ij}^{6}(r_{ij})\frac{C_{ij}^{6}}{r_{ij}^{6}} - f_{ij}^{8}(r_{ij})\frac{C_{ij}^{8}}{r_{ij}^{8}} \qquad (16)$$

where C_{ij}^6 and C_{ij}^8 are the dispersion coefficients and $f_{ij}^{(n)}$ are dispersion damping functions given by

$$f_{ij}^{(n)}(r_{ij}) = 1 - e^{-(b_{ij} r_{ij})} \sum_{k=0}^{n} \frac{(b_{ij} r_{ij})^k}{k!} \qquad (17)$$

with $k = 4$ for dipole polarization, and 6 for the C_8 term. The polarization parts of the potential include chloride ion polarization only.[6] We used a chloride ion polarizability of 20.0 au and applied a damping function

$$g_{ij}(r_{ij}) = 1 - c_{ij}^{D}\, e^{-(b_{ij}^{D} r_{ij})} \sum_{k=0}^{4} \frac{(b_{ij}^{D} r_{ij})^k}{k!} \qquad (18)$$

to the interaction between the anion dipoles and the cation charges. The potential parameters are detailed in Table 3.

References and Notes

(1) *A Technology Roadmap for Generation IV Nuclear Energy Systems*; US DOE NERAC/GIF: Washington, DC, 2002; online at http://gif.inel.gov/roadmap/pdfs/gen_iv_roadmap.pdf.
(2) Nash, K. L.; Lumetta, G. J.; Clark, S. B.; Friese, J. I. *ACS Symp. Ser.* **2006**, *933*, 3−20.
(3) See e.g. http://en.wikipedia.org/wiki/PUREX.
(4) Le Brun, C. *J. Nucl. Mater.* **2007**, 360, 1−5.
(5) Noskov, S. Y.; Berneche, S.; Roux, B. *Nature* **2004**, *431*, 830.
(6) Hutchinson, F.; Wilson, M.; Madden, P. A. *Mol. Phys.* **2001**, *99*, 811−824.
(7) Glover, W. J.; Madden, P. A. *J. Chem. Phys.* **2004**, *121*, 7293−7303.
(8) Okamoto, Y.; Madden, P. A.; Minato, K. *J. Nucl. Mater.* **2005**, *344*, 109−114.
(9) Lantelme, F.; Cartailler, T.; Berghoute, Y.; Hamdani, M. *J. Electrochem. Soc.* **2001**, *148*, C604−C613.
(10) Cassayre, L. Malmbeck, R.; Masset, P.; Rebizant, J.; Serp, J.; Soucek, P.; Glatz, J.-P. *J. Nucl. Mater.* **2007**, *360*, 49−57.
(11) Rycerz, L.; Gadzuric, S.; Gong, W.; Ingier-Stocka, E.; Gaune-Escard, M. *J. Mol. Liq.* **2007**, *131−132*, 246−253.
(12) Conocar, O.; Douyère, N.; Lacquement, J. *J. Alloys Compd.* **2005**, *389*, 29−33.
(13) Martin R. A. *Electronic Structure: Basic Theory and Practical Applications*; Cambridge University Press: Cambridge, 2004.
(14) Kohanoff, J. J. *Electronic Structure Calculations for Solids and Molecules*; Cambridge University Press: Cambridge, 2006.
(15) Frenkel, D.; Smit, B. *Understanding Molecular Dynamics: From Algorithms to Applications*, 2nd ed.; Academic Press: London, 2002.
(16) Ferrario, M.; Ciccotti, G.; Spohr, E.; Cartailler, T.; Turq, P. *J. Chem. Phys.* **2002**, *117*, 4947−4953.
(17) Sanz, E.; Vega, C. *J. Chem. Phys.* **2007**, *126*, 014507.

(18) Martyna, G. J.; Tuckerman, M. E.; Tobias, D. J.; Klein, M. L. *Mol. Phys.* **1996**, *87*, 1117−1157.

(19) Barin, I. *Thermochemical data on pure substances*; VCH: Weinheim, Germany, 1989.

(20) Plambec, J. A. *Encyclopedia of electrochemistry of the elements Vol X: Fused salt systems*; Bard, H. J., Ed.; Marcel Dekker: New York, 1976.

(21) Yamana, H.; Wakayama, N.; Souda, N.; Moriyama, H. *J. Nucl. Mater*. **2000**, *278*, 37−47.

(22) Masset, P.; Konings, R. J. M.; Malmbeck, R.; Serp, J.; Glatz, J.-P. *J. Nucl. Mater.* **2005**, *344*, 173−179.

(23) Fusselman, S. P.; Roy, J. J.; Grimmett, D. L.; Grantham, L. F.; Krueger, C. L.; Nabelek, C. R.; Storvick, T. S.; Inoue, T.; Hijikata, T.; Kinoshita, K.; Sakamura, Y.; Uozumi, K.; Kawai, T.; Takahashi, N. *J. Electrochem. Soc.* **1999**, *146*, 2573−2580.

(24) Roy, J. J.; Grantham, L. F.; Grimmett, D. L.; Fusselman, S. P.; Krueger, C. L.; Storvick, T. S.; Inoue, T.; Sakamura, Y.; Takahashi, N. *J. Electrochem. Soc.* **1996**, *143*, 2487−2492.

(25) Chamelot, P.; Massot, L.; Hamel, C.; Nourry, C.; Taxil, P. *J. Nucl. Mater.* **2007**, *360*, 64−74.

(26) Aguado, A.; Bernasconi, L.; Jahn, S.; Madden, P. A. *J. Chem. Soc., Faraday Discuss*. **2003**, *124*, 171−184.

(27) Madden, P. A.; Heaton, R. J.; Aguado, A.; Jahn, S. *J. Mol. Struct.: THEOCHEM* **2006**, *771*, 9−18.

(28) Salanne, M.; Simon, C.; Turq, P.; Heaton, R.J.; Madden, P. A. *J. Phys. Chem. B* **2006**, *110*, 11461−11467.

(29) Heaton, R. J.; Brookes, R.; Madden, P. A.; Salanne, M.; Simon, C.; Turq, P. *J. Phys. Chem. B* **2006**, *110*, 11454−11460.

(30) Data from WebElements; www.webelements.com.